

29 Abstract

30 Determining phylogenetic relationships among recently diverged species has long been
31 a challenge in evolutionary biology. Cytoplasmic markers, which have been widely used
32 notably in the context of molecular barcoding, have not always proved successful in
33 resolving such phylogenies, but phylogenies for closely related species have been
34 resolved at a much higher detail in the last couple of years with the advent of next-
35 generation-sequencing technologies and associated techniques of reduced genome
36 representation. Here we examine the potential and limitations of one of such techniques
37 — Restriction-site Associated DNA (RAD) sequencing, a method that produces
38 thousands of (mostly) anonymous nuclear markers, in disentangling the phylogeny of
39 the fly genus *Chiastocheta* (Diptera: Anthomyiidae). This genus encompasses seven
40 described species of seed predators, which have been widely studied in the context of
41 their ecological and evolutionary interactions with the plant *Trollius europaeus*
42 (Ranunculaceae). So far, phylogenetic analyses using mitochondrial markers failed to
43 resolve monophyly of most of the species from this recently diversified genus,
44 suggesting that their taxonomy may need to be revised. However, relying on a single,
45 non-recombining molecule and ignoring potential incongruences between
46 mitochondrial and nuclear loci may provide incomplete account of a lineage history. In
47 this study, we apply both classical Sanger sequencing of three mtDNA regions and RAD-
48 sequencing, for reconstructing the phylogeny of the genus. Contrasting with results
49 based on mitochondrial markers, RAD-sequencing analyses retrieved the monophyly of
50 all seven species, in agreement with the morphological species assignment. We found
51 robust nuclear-based species assignment of individual samples, and low levels of
52 estimated contemporary gene flow among them. However, despite recovering species'

53 monophyly, interspecific relationships varied depending on the set of RAD loci
54 considered, producing contradictory topologies. Moreover, coalescence-based
55 phylogenetic analyses revealed low supports for most of the interspecific relationships.
56 Our results indicate that despite the higher performance of RAD-sequencing in terms of
57 species trees resolution compared to cytoplasmic markers, reconstructing inter-specific
58 relationships may lie beyond the possibilities offered by large sets of RAD-sequencing
59 markers in cases of strong gene tree incongruence.

60

61 Keywords: coalescent analysis; DNA barcoding; maximum likelihood; mito-nuclear
62 incongruence; single nucleotide polymorphisms; quartet inference

63

64 1. Introduction

65 Recently diverged lineages pose a problem for traditional phylogenetic approaches that
66 typically rely on a small set of relatively slowly evolving loci (DeFilippis 2000), often
67 lacking resolution at narrower evolutionary scales (Cariou et al. 2013). In addition,
68 complex processes such as incomplete lineage sorting (Avisé et al. 2008; Maddison &
69 Knowles 2006; Pollard et al. 2006) and gene flow among species (Leaché et al. 2013)
70 increase incongruences among gene trees and topological deviations from the species
71 tree (Degan & Rosenberg 2009; Maddison 1997). This is especially true for lineages
72 that have undergone rapid radiations, in which ancestral polymorphisms sorted
73 idiosyncratically into the descendant taxa through short evolutionary nodes (Avisé et al.
74 2008), and in cases where subsequent evolutionary events may blur phylogenetic signal
75 (Whitfield & Kjer 2008; Whitfield & Lockhart 2007). Sampling more loci has been
76 shown to be a promising approach in such cases (Rokas & Carroll 2005; Townsend et al.
77 2011; Wielstra et al. 2014; Williams et al. 2013), but the spectrum of genetic markers
78 developed for phylogeny estimation is still limited (Whitfield & Kjer 2008).

79 Next-generation sequencing approaches, particularly reduced representation genome
80 sequencing (Davey et al. 2011), offer the possibility to sample thousands of genomic
81 markers from non-model species. Among them, Restriction site-Associated DNA (RAD;
82 Baird et al. 2008) techniques rely on the sequencing of short DNA fragments flanking
83 restriction sites, generating random anonymous genomic markers, homologous across
84 the analyzed samples (Andrews et al. 2016; Davey & Blaxter 2010). From a phylogenetic
85 perspective, an important aspect of RAD markers is the rise in the proportion of ‘null
86 alleles’ as genome divergence across samples increases. This phenomenon is caused by
87 random mutations occurring in the restriction sites that decrease the numbers of

88 shared RAD loci among taxa, resulting in data matrices containing large amounts of
89 missing data (Cariou et al. 2013; Chattopadhyay et al. 2014; Gautier et al. 2013).
90 However, using an in-silico approach Rubin et al. (2012) and Cariou et al. (2013) have
91 shown that RAD-seq data can be used successfully to resolve species relationships that
92 transcend timescales up to 60 Mya (million years ago). Experimentally sampled RAD
93 datasets have been applied to reconstruct phylogenetic relationships, mostly among
94 recently diverged taxa (e.g., Eaton & Ree 2013; Harvey et al. 2016; Jones et al. 2013;
95 Leaché et al. 2015; Nadeau et al. 2013; Wagner et al. 2013), with fewer studies involving
96 more distantly related ones, even up to even 80 Mya (e.g., Cruaud et al. 2014; Eaton et
97 al. 2016; Herrera and Shank 2016; Hipp et al. 2014; Pante et al. 2015). Although these
98 genomic datasets improved phylogenetic inferences for groups that were ambiguous
99 using classical markers (e.g., Escudero et al. 2014; Hipp et al. 2014), the potential utility
100 of RAD loci for resolving more complex phylogenetic histories, such as those where
101 historical introgression has occurred or those associated with incomplete lineage
102 sorting, remains still poorly explored (Combosch & Vollmer 2015; Eaton & Ree 2013).
103 Moreover, the use of RAD datasets as markers for evolutionary genetics has recently
104 been heavily discussed (Lowry et al. 2017; McKinney et al. 2017).
105 In this study, we test the utility of RAD-sequencing to recover phylogenetic
106 relationships in a genus of seed parasitic pollinators of *Trollius europaeus*
107 (Ranunculaceae) — flies from the genus *Chiastocheta* Pokorny, 1889 (Diptera:
108 Anthomyiidae). Here, sequencing of mitochondrial markers failed to reveal the
109 monophyly and phylogenetic relationships among previously morphologically
110 described species (Després et al. 2002; Espíndola et al. 2012). This discordance
111 between morphology and mitochondrial phylogeny has been interpreted as a call for a

112 taxonomic revision, and a possible reconsideration of conclusions from previous
113 ecological and evolutionary studies (Espíndola et al. 2012). However, several
114 mechanisms may cause mitochondria not to track species evolution (Funk & Omland
115 2003) and, indeed, there are many cases where mitochondrial and nuclear gene trees
116 have been shown to be incongruent (e.g., Govindarajulu et al. 2015; Phillips et al. 2013;
117 Seehausen et al. 2003). As relying on a single, non-recombining molecule may provide a
118 misleading account of a species history (Ballard & Whitlock 2004), utilizing a large set
119 of independent nuclear loci (sampled through RAD-sequencing) should allow us to test
120 the monophyly of the morphologically described species and resolve phylogenetic
121 relationships among them. Whether or not molecular markers are able to reveal
122 scenarios of rapid radiations is still an open question (Giarla & Esselstyn 2015). In
123 these, identifying a single species tree might lie beyond analytical possibilities due to
124 pervasive conflicts among the gene trees, particularly when population sizes are large
125 and speciation events happen at a higher rate than the mutation-drift equilibrium,
126 eventually producing conflicting topologies. In order to explore gene and species trees,
127 we applied both a concatenation-based phylogenetic approach (i.e., RAxML; Stamatakis
128 2014) and a coalescence-based inference method (i.e., SVDquartets; Chifman & Kubatko
129 2014) to a RAD-seq dataset encompassing specimens from 51 European populations,
130 representative of the seven recognized *Chiastocheta* morphospecies. In order to
131 examine the extent to which different combinations of RAD loci may produce distinct
132 species trees, we used a newly developed algorithm that performs loci binning, using
133 dissimilarity levels among phylogenetic patterns retrieved at single loci (treeCl; Gori et
134 al. 2016). We also applied population genetics clustering algorithms (i.e., STRUCTURE;
135 Pritchard et al. 2000) as a control. Eventually, we compared our results to those

136 obtained with classical phylogenetic inference based on concatenation of three
137 mitochondrial regions.

138 2. Materials and methods

139 2.1 Study system

140 The center of origin and diversity of *Chiastocheta* has been inferred to be the Western
141 Palearctic, where seven fly species are involved in nursery pollination interactions with
142 *Trollius europaeus* L. (Espíndola et al. 2012; Pellmyr 1989, 1992; Suchan et al. 2015).
143 These seven morphologically delimited European *Chiastocheta* species, namely *C.*
144 *dentifera* Hennig 1953; *C. inermella* (Zetterstedt, 1838); *C. lophota* Karl, 1943; *C.*
145 *macropyga* Hennig, 1953; *C. rotundiventris* Hennig, 1953; *C. setifera* Hennig, 1953 and *C.*
146 *trollii* (Zetterstedt, 1838) are ecologically very similar and often sympatric (Collin 1954;
147 Hennig 1976; Michelsen 1985; Zetterstedt 1845; V. Michelsen pers. comm.). In his
148 monograph of this plant-pollinator interaction, Pellmyr (1992) discussed another
149 species, *C. abruptiventris* as a northern vicariant of *C. rotundiventris*, a taxon not
150 supported by previous molecular studies (Espíndola et al. 2012) and never formally
151 described. Although all *Chiastocheta* reproduce within the flowers of *T. europaeus*, with
152 potential cross-species mating possibilities, no putative hybrids have been observed
153 based on genital morphology (T. Suchan and A. Espíndola, pers. obs.).
154 Although the species are well defined morphologically, mitochondrial phylogenies
155 recovered only three monophyletic clades – *C. rotundiventris*, *C. dentifera*, and *C. lophota*
156 (Després et al. 2002; Espíndola et al. 2012), and suggested a polyphyletic origin for *C.*
157 *inermella* and *C. setifera* (Després et al. 2002; Espíndola et al. 2012), with *C. macropyga*
158 and *C. trollii* being paraphyletic (Espíndola et al. 2012). Molecular dating placed the

159 most recent common ancestor of all European species at the end of the Pliocene (2-3.4
160 Ma; Després et al. 2002; Espíndola et al. 2012), and indicated that most diversification
161 events occurred within the last 1.6 Ma.

162 2.2 Sampling

163 *Chiastocheta* specimens were sampled from 51 European populations during spring and
164 summer 2006, 2007, and 2008 (Table 1; maps on Fig. S1). The flies were killed and
165 preserved in 70% ethanol and stored at room temperature until DNA extraction.
166 Collected specimens were identified to morphospecies following Hennig (1976) and
167 unpublished keys (V. Michelsen). All identifications were confirmed by an expert (V.
168 Michelsen, Natural History Museum of Denmark, Copenhagen), as the taxonomical
169 revision of the genus is not yet published.

170 2.3 Sequencing mitochondrial regions and RAD markers

171 DNA was extracted from insect legs using a DNeasy Blood and Tissue Kit (Qiagen,
172 Hilden, Germany), following the manufacturer's instructions. We amplified three
173 mitochondrial regions: COI, COII, and the ultra-variable D-loop (control) region. We
174 followed Espíndola et al. (2012) for sequencing of the COI and COII regions. For D-loop
175 we used primers TM-N-193 and SR-J-14612 as described in Simon et al. (1994) as
176 described by Espíndola et al. (2012) with the following modification of the PCR
177 program: 5 min at 95°C, followed by 35 cycles of 1 min at 95°C, 1 min of annealing
178 at 55°C and 2 min of elongation at 60°C, and 5 min of final elongation at 60°C. PCR
179 products were sequenced at Macrogen Inc. (South Korea) and FASTERIS SA (Switzerland).
180 Chromatograms were visually corrected on ChromasPro 1.41 (Technelysium Pty. Ltd.).
181 Alignment was performed using MUSCLE algorithm (Edgar 2004) in Geneious 10.1.3

182 (Biomatters, Auckland, New Zealand) and gaps with more than 50% missing data in the
183 D-loop region were removed. Additionally, a dataset with D-loop removed was
184 analyzed. Double digest RAD (ddRAD) libraries were prepared according to Mastretta et
185 al. (2014), a modified protocol of Peterson et al. (2012), without performing the size-
186 selection of DNA fragments, and other minor modifications (see Supporting
187 Information). The enzymes used for DNA digestion were SbfI and MseI. Libraries were
188 sequenced at the Lausanne Genomic Technologies Facility (Switzerland) on three lanes
189 of the HiSeq2500 instrument (Illumina, San Diego, USA) using a 2x100 bp paired-end
190 reads protocol. For RAD-sequencing we introduced technical replicates for optimizing
191 *de novo* assembly and controls for the effects of sequencing errors and allele dropout on
192 the final results (Mastretta-Yanes et al. 2015; samples with “REPL” suffix in Table S1),
193 and DNA extraction replicates from the fly thoracic muscle (in order to control for flies’
194 body contamination with pollen; samples with “MUS” suffix in Table S1).

195 2.4 RAD-seq loci assembly

196 Two important considerations for *de novo* RAD loci assembly are the parameters for
197 clustering orthologous loci, while filtering out paralogs (Eaton 2014; Mastretta et al.
198 2015). If the sequence similarity required to consider sequence as orthologs is set too
199 high, real heterozygous alleles will be split into more than one cluster, therefore
200 creating false homozygous loci (Harvey et al. 2015). On the other hand, if the similarity
201 is set too low, this will result in paralogous sequences being clustered together. Several
202 methods were proposed for filtering out such sequences from the final dataset,
203 including ploidy filtering (removing clusters that have more than two sequences per
204 individual) and filtering out highly variable loci (Eaton 2014; Ilut et al. 2014). As there

205 are no general guidelines for fine-tuning the parameters mentioned above, we
206 empirically tested how the different clustering parameters affected the final dataset.
207 Finally, we chose the dataset with clustering parameter that maximized the loci overlap
208 between pairs of technical replicates (see below). Loci overlap among samples and pairs
209 of technical replicates were calculated using the RADami 1.0 library in R (Hipp et al.
210 2014).

211 Read demultiplexing and *de novo* assembly of RAD loci was performed using the pyRAD
212 3.0.1 package (Eaton 2014), based on an alignment-clustering algorithm. This approach
213 allows for indel variation among more diverged specimens. Moreover, it also allows for
214 lower similarity among the clustered reads, making it well-suited for phylogenetic-scale
215 analyses. First, the reads were demultiplexed according to the in-line 6-nucleotides
216 barcode present at the beginning of each sequenced fragment, while allowing for one
217 mismatch. Only reads with the restriction site present were retained for further
218 analyses. All nucleotides with Phred quality score lower than 20 were converted to
219 unknown bases and reads with more than four unknown sites were removed from the
220 dataset. Reads were then clustered within and between individuals, with a minimum
221 number of six reads to form a cluster and sequence similarity of 75%, 80%, 85%, 90%,
222 and 95%. Possible clustered paralogs or repetitive sequences were removed by filtering
223 out the loci that had more than five variable positions per locus or more than 10 shared
224 polymorphic sites in a locus among individuals, and the loci for which more than two
225 alleles were present per individual. Finally, datasets were produced by retaining the loci
226 present in a minimum of 10, 20, and 100 individuals and compared for the total number
227 of loci, proportion of missing data, loci overlap among replicates, and the mean number
228 of individuals per locus.

229 2.5 Phylogenetic analyses

230 We performed Maximum-likelihood (ML) analyses using RAxML (Stamatakis 2014)
231 with rapid bootstrap analyses and extended majority-rule consensus tree automatic
232 bootstrap stopping criterion, following search for the best-scoring ML tree. The
233 mitochondrial regions were partitioned using the PartitionFinder 2.1.1 software
234 (Lanefar et al. 2016). Analyses were performed in the RAxML 8.2.4, for the
235 mitochondrial dataset. For the dataset consisting of COI, COII, and D-loop regions the
236 GTR+G+I model with all three nucleotide positions on coding genes considered as
237 separate partitions and D-loop as a fourth partition. For the dataset consisting of COI
238 and COII the GTR+G model with the first two nucleotide positions considered as a first
239 and third nucleotide position considered as a second partition. Analyses for the RAD
240 dataset were performed using the GTRCAT model in the RAxML 8.2.10 version on the
241 CIPRES cluster (San Diego CA, USA; Miller et al. 2010). For the RAD-based dataset,
242 replicated samples were retained in the phylogenetic analyses and the concatenated
243 matrix was considered as a single partition. Additionally, ML analyses of the RAD
244 datasets with other clustering parameters were performed in order to evaluate how this
245 parameter affects the tree topology. The trees were rooted with *C. rotundiventris* as an
246 outgroup, as identified previously (Després et al. 2002; Espíndola et al. 2012).
247 To account for the effects of incongruence among nuclear loci on the inferred
248 phylogenies — for instance resulting from incomplete lineage sorting, we applied the
249 method of Gori et al. (2016) implemented in the treeCl package (<http://git.io/treeCl>).
250 Because the majority of RAD loci had sparse coverage over the individuals, we kept only
251 loci present in more than 100 individuals for this part of analysis. The ML
252 phylogenies were first calculated for every locus using the GTR+G model as

253 implemented in RAxML 8.1.11 (Stamatakis 2014). Then, pairwise geodesic distances
254 between all the resulting single-locus phylogenies were measured, and the trees were
255 grouped based on the distance matrix using spectral clustering (a protocol hereafter
256 referred to as binning). The number of bins was estimated using the nonparametric
257 bootstrapping stopping criterion. Support for each branch in each topology was
258 calculated using aBayes in PhyML (Anisimova et al. 2011). We also analyzed the log-
259 likelihood improvement when analyzing the data with $n+1$ splits vs. n splits, compared
260 to the null expectation (i.e. random loci clustering).

261 Additionally, we applied a coalescent-based inference method using SVDquartets
262 (Chifman and Kubatko 2014) as implemented in PAUP* v.4a150 and v.4a151 (Swofford
263 2002). This method infers the topology among randomly sampled quartets using a
264 coalescent model, and assembles the randomly sampled quartets using a quartet
265 amalgamation method. Breaking the sequence into quartets makes the analysis of large
266 numbers of loci feasible. We randomly sampled the maximum of all possible quartets
267 (i.e. 48,603,900 quartets = 200 taxa) with the multispecies coalescent option and 1,000
268 bootstrap replicates. The quartets were summarized with the QFM (Reaz et al. 2014)
269 quartet amalgamation program as implemented in PAUP*. Phylogenetic trees were
270 visualized using the ape 3.2 R package (Paradis et al. 2004).

271 2.6 Population structure

272 We inferred population structure using the admixture model implemented in
273 STRUCTURE 2.3.4 (Pritchard et al. 2000), without prior population assignment and with
274 allele frequencies correlated among populations. The software uses a Bayesian
275 framework to estimate the likelihood of the data given a number of *a priori* defined K

276 population clusters, outputting the likelihood of each sample to belong to each possible
277 cluster. This analysis was performed after removing technical replicates from the
278 dataset, retaining only the loci present in a minimum of 20 individuals, and selecting
279 one random single SNP from each locus. Analyses were run for K values ranging
280 between 1 and 8, with a burn-in of 200K cycles, followed by 1M cycles of sampling, with
281 3 replicates for each K value. The optimal K value was identified following Evanno et al.
282 (2005), as implemented in STRUCTURE HARVESTER (Earl & vonHoldt 2012). To
283 account for the phylogenetic component in the missing alleles, we ran STRUCTURE with
284 the recessive alleles model, with missing data coded as recessive.

285 3. Results

286 3.1 *Chiastocheta* sampling

287 We analyzed a total of 272 *Chiastocheta* specimens sampled from the entire European
288 range of the genus (see Table 1 and Fig. S1 for maps of the sampled specimens). Most
289 species displayed a broad spatial distribution. Up to six species could be found in one
290 single locality during a single visit (Table 1, mean = 2.7 species per locality, SD = 1.5),
291 confirming the sympatric nature of the species and the existing opportunities for
292 hybridization.

293 3.2 Sequencing and RAD loci assembly results

294 After initial screening, 21 samples were removed from the final dataset because of
295 insufficient coverage or technical errors. We successfully analyzed 260 specimens for
296 the mitochondrial dataset (255 for COI, 204 for COII, 141 for the first, and 152 for the
297 second fragment of the D-loop), and 263 for the RAD dataset, while 251 samples were

298 shared between the datasets (Table 1). For the RAD dataset, we also sequenced 22
299 technical replicates (samples with “REPL” suffix in Table S1), and 11 DNA extraction
300 replicates from the fly muscle vs. extractions from legs (samples with “MUS” suffix in
301 Table S1).

302 Sequencing of the mitochondrial regions yielded 1132 nucleotide positions for the
303 COI+COII dataset (of which 120 were variable) and 2003 for the COI+COII+D-loop
304 dataset (of which 334 were variable), after alignment and gap filtering. Three runs of
305 RAD sequencing output 552’425’482 of 2 x 100 bp reads, from which 340’598’636
306 (62%) passed the restriction site and barcode quality filters (Table S1).

307 After comparing the number of loci, coverage, and overlap of loci among replicates in
308 the obtained datasets (Fig. S2), we chose the dataset with a minimum of 75% sequence
309 similarity required for the sequences to cluster in a locus and a minimum of 20
310 individuals per locus for the main analyses. This dataset contained 1724 loci after
311 filtering and paralog removal, with 82’782 variable sites. The proportion of missing data
312 in the dataset was 0.84, with a strong phylogenetic component in the distribution of
313 missing loci (Fig. S3a). After sampling one SNP per locus for the STRUCTURE analysis,
314 we obtained 1669 SNPs, of which 159 were bi-allelic.

315 For the dataset used for assessing loci incongruence in the RAD-seq based phylogeny
316 (see below), we focused on loci present in at least 100 individuals. This resulted in a
317 matrix of 176 loci (among 1724 overall number of loci identified; i.e., 10.2%) with
318 missing data showing much less phylogenetic structuring (Fig. S3b).

319 3.3 Mitochondrial and nuclear-data phylogenies

320 The mitochondrial phylogeny on the COI+COII_D-loop dataset (Fig. 1a and Fig. S4a)
321 failed to resolve four of the clades identified based on the RAD-seq data (see below), but
322 retrieved well-supported monophyletic group for *C. rotundiventris* and, to the lesser
323 extent for *C. dentifera* and *C. inermella*, as both of the latter had two specimens placed
324 outside their clades. *C. inermella*, *C. setifera*, and *C. trollii* formed one clade with the
325 species extensively interdispersed and a clade containing mostly *C. macropyga* nested
326 within. As the analysis based based on the reduced COI+COII dataset recovered a similar
327 pattern, except placing *C. lophota* as sister to *C. macropyga*, we refer to the results of the
328 larger dataset in the rest of the paper. Most of the *C. lophota* samples also formed one
329 clade with lower support values. The relationships among samples from the remaining
330 four morphospecies remained unresolved, without clear support for the
331 morphologically described species.

332 In contrast to the ML mtDNA phylogeny, both ML and SVDquartets analysis of the RAD
333 analysis (Fig. 1b, c and Fig. S4b, c) confirmed monophyly of the seven morphologically
334 defined taxa. RAxML analysis revealed relatively high bootstrap supports (> 90%) for
335 all of the interspecific relationships, except the split between *C. setifera* and the clade (*C.*
336 *lophota*, (*C. macropyga*, (*C. dentifera*, *C. trollii*))) with bootstrap support > 80%. The split
337 of *C. rotundiventris* into two putative vicariant clades, informally proposed by Pellmyr
338 (1992) — northern *C. abruptriventris* and southern *C. rotundiventris*, was not recovered.
339 SVDquartets analysis also confirmed monophyly of the species, but only the split
340 between *C. dentifera* and *C. trollii* had a bootstrap support > 90%; the clade (*C.*
341 *macropyga*, (*C. dentifera*, *C. trollii*)) had bootstrap support > 80%; these two clades were
342 the only ones supported by both SVDquartets and the RAxML analyses (Fig. 1c).

343 Moreover, SVDquartets revealed two well-supported clades within *C. rotundiventris*.
344 These however do not show any pattern of vicariance and often occur together in a
345 single population, thus most likely do not correspond to the two vicariant species of *C.*
346 *abruptiventris* and *C. rotundiventris* as discussed by Pellmyr (1992). The technical
347 replicates were consistent in the placement of the sample within the proper clade, and
348 most replicates were placed as sister clades with both methods (Fig. S4b,c).

349 3.4 Incongruence among the RAD-sequencing loci

350 TreeCl analysis identified, in the most conservative interpretation, at least four clusters
351 of loci, as the largest likelihood improvement was obtained when increasing the number
352 of bins from three to four (Fig. S6). The bin sizes were of 29, 42, 47, and 58 loci,
353 therefore the identified groups were not simply consisting of a few outliers. The trees
354 inferred for the four bins confirmed the monophyly of the analysed species to a large
355 extent, although few individuals appeared outside their expected clades. The largest
356 departure from monophyly was observed for *C. lophota* in the smallest tree consisting of
357 29 loci (Fig. 2). The trees inferred for each cluster had branch supports for interspecific
358 nodes larger than 95%, and differed substantially in terms of topology and branch
359 lengths. Only one tree, with the largest number of loci (i.e., 58) supported the only clade
360 that was supported by both RAML and SVDquartets analysis (*C. macropyga*, (*C.*
361 *dentifera*, *C. trollii*)). Except that, the interspecific relationships retrieved with each of
362 the treeCl bins were different than with the concatenated RAxML analysis and
363 SVDquartets analysis (Fig. 1b, c).

364 3.5 Structure analysis

365 We found low levels of contemporary introgression, as shown by STRUCTURE analysis.
366 The most likely K number of STRUCTURE groups was consistent with the number of
367 morphological species (7), and all samples were assigned to their ‘correct’
368 morphospecies (Fig. 1d). Also for lower numbers of clusters, we did not observe
369 signatures of introgression (Fig. S5).

370 4. Discussion

371 4.1 Utility and limits of RAD-sequencing for resolving phylogeny of 372 a „difficult” genus

373 RAD-sequencing successfully discriminated all formally described European
374 *Chiastocheta* species. The robust species delineation is striking when compared to
375 mtDNA-based trees that failed to support monophyly of *C. inermella*, *C. macropyga*, *C.*
376 *setifera*, and *C. trollii* (Fig. 1a and Fig. S4a; see also: Després et al. 2002; Espíndola et al.
377 2012). The ability to recover previously defined morphological species in our dataset,
378 whatever analysis method used (i.e., maximum-likelihood phylogenetic reconstruction
379 using a concatenated matrix with RAxML, coalescence-based phylogenetic inference
380 with SVDquartets, or population-genetics clustering with STRUCTURE), supports the
381 results of a previous simulation study by Hovmöller et al. (2013), that high amounts of
382 missing data, typical for RAD-based datasets, should not interfere with clade (or cluster)
383 identification. Recently, similar conclusions were drawn by Eaton et al. (2016)
384 concerning the SVDquartets method.

385 In contrast, no consensus could be reached in retrieving inter-specific relationships.
386 Whereas RAxML identified relationships with high bootstrap support in four of the five
387 possible interspecific relationships, only two of them were also supported by the
388 SVDquartets analysis (Fig. 1b,c). Incongruence in the phylogenetic signals associated
389 with different sets of loci could explain the difficulty in resolving these interspecific
390 relationships. When performing loci binning using treeCL (Gori et al. 2016), we found
391 out that different subsets of loci (in our case, the optimal number of bins was equal to
392 four) produced different topologies, while still being largely congruent in the sample
393 assignment into species (Fig. 2).

394 Short interspecific branches in the resolved phylogenies confirm the conclusions of
395 Espíndola et al. (2012) that most of the species from the *Chiastocheta* genus underwent
396 a recent (less than 1.6 Mya), rapid radiation. These results highlight the fact that in such
397 cases it may be impossible to retrieve some of the phylogenetic relationships among the
398 taxa as fully bifurcating tree, because gene trees may depict different evolutionary
399 histories due to incomplete lineage sorting (Avice et al. 2008; Maddison 1997). This is a
400 limitation shared with classical markers (Walsh et al. 1999) and other NGS approaches
401 (see below), pointing to a possible constitutive limitation in resolving rapid radiations.

402 In rapidly diverging taxa, even the large number of nuclear markers, while being more
403 successful here in recovering species boundaries than mitochondrial markers may not
404 be informative-enough to retrieve all interspecific evolutionary relationships.

405 The extent to which the above limitation is the result of technical constraints of RAD
406 datasets or a true biological limitation remains to be investigated. RAD-seq targets
407 random, mostly neutral parts of the genome. This results in high number of lineage-
408 specific mutations that bear a strong signal to delineate species or populations – within

409 these fast-evolving parts of the genome, even varying allele copy-numbers (i.e. recent
410 paralogs) can appear as population-specific (Mastretta-Yanes et al. 2014). The
411 downside is however, missing data increases rapidly with evolutionary distance as a
412 result of the loss of restriction sites (Cariou et al. 2013; Chattopadhyay et al. 2014;
413 DaCosta & Sorenson 2016; Gautier et al. 2013; Rubin et al. 2012; Wagner et al. 2013).
414 For instance, Leaché et al. (2015) found differences between phylogenies obtained
415 using RAD-seq vs. target enrichment techniques, whereas other studies have shown the
416 agreement among data types (Manthey et al. 2016). The latter techniques rely on
417 capture of a predefined (Faircloth et al. 2014; McCormack et al. 2012) or random
418 (Suchan et al. 2016, Schmid et al. 2017) subset of loci. By not relying on the presence of
419 restriction sites, and thus having less missing data, enrichment techniques may be
420 better suited for broader phylogenetic scales.

421 Nevertheless, it has been shown that even with hundreds of conserved loci, known
422 substitution models and several individuals per species, trees with short branches are
423 difficult to resolve, and ML analyses based on concatenated sequences may provide high
424 bootstrap values despite incorrectly resolved topologies (Giarla & Esselstyn 2015;
425 Kubatko & Degnan 2007; but see Gatesy & Springer 2013; Springer & Gatesy 2016; Roch
426 & Warnow 2015). This is exemplified by our study, in which using all RAD loci, we
427 obtained a ML phylogeny with highly supported interspecific nodes, whereas
428 coalescence-based phylogenetic inference did not show strong supports for most of the
429 interspecific relationships. Our exploration of explanations for such a discrepancy using
430 the loci binning approach showed support for at least four different underlying gene
431 tree topologies. In these analyses, we reduced the dataset to a non-random set of loci
432 when filtering for high loci coverage among samples. The retained loci, present in at

433 least 100 analyzed individuals, and with less phylogenetically-structured missing data
434 (see Fig. S3b), should be characterized by lower mutation rates or being under
435 stabilizing selection (Huang & Knowles 2014). Using binning, the best fit to the data was
436 not obtained with a single bin of loci but with four. We could therefore not identify one
437 single evolutionary history of the *Chiastocheta* genus, but rather equally-supported
438 gene trees topologies. Importantly, these different topologies cannot be attributed to a
439 few outlier loci, as their distribution was relatively even across the clusters (29, 58, 42
440 and 47 loci; Fig. S6), incongruence among these sets possibly impacting maximum-
441 likelihood phylogenetic reconstruction using a concatenated matrix and coalescence-
442 based phylogenetic inference. We have also confirmed that in such cases, ML methods
443 provide elevated bootstrap support values, and that lower bootstrap support values
444 resulting from coalescence-based methods may better reflect the biological uncertainty
445 of interspecific relationships.

446 4.2 Mitonuclear discordance in the phylogeny of *Chiastocheta*

447 While our RAD-sequence dataset delineated seven clades, with full agreement with the
448 morphological assignments, mitochondrial data failed to support species monophyly,
449 except for *C. rotundiventris* and, to a lesser extent, *C. lophota* and *C. dentifera*. The other
450 remaining species: *C. inermella*, *C. setifera* and *C. trollii* formed a large clade with the
451 species extensively interdispersed and with the clade consisting mostly of *C. macropyga*
452 nested within (Fig. 1a). Despite, on average, mitochondrial markers should be more
453 suited for capturing relationships among recently diverged lineages, due to an effective
454 population size four times less than that of nuclear genes (assuming neutral processes,
455 equal sex ratios, and unbiased mating systems), and thus shorter coalescence times

456 (Zink & Barrowclough 2008), analyzing a large dataset of nuclear markers provided
457 more power to discriminate the species in our case.

458 Mitonuclear discordance patterns can be explained either by the different biological
459 properties of mitochondrial DNA (vegetative segregation, uniparental inheritance,
460 intracellular selection, and reduced recombination; Birky 2001) or differences in the
461 evolutionary histories of nuclear and mitochondrial markers [e.g., direct selection on
462 the mitochondrial genes (Ballard et al. 2007; Ballard & Pichaud 2014; Boratyński et al.
463 2014; Dowling et al. 2008), incomplete lineage sorting, historical or ongoing gene flow
464 among species, or hybrid speciation]. Indeed, it has been shown before that relying on a
465 single, non-recombining mtDNA molecule may provide a misleading account of a
466 species history (e.g., Ballard & Whitlock 2004; Govindarajulu et al. 2015; Phillips et al.
467 2013; Seehausen et al. 2003; and reviews by Funk & Omland 2003; Rubinoff & Holland
468 2005). While investigating the reasons for the mito-nuclear discordance was not within
469 the scope of this paper, we could reject the hypothesis of a contemporary gene flow or
470 hybrid origin of the taxa as responsible for this pattern. We did not detect signature of a
471 genetic mosaic in the—mostly—nuclear RAD data, which would be expected in the case
472 of hybrid origin (Ballard 2000; Brelsford et al. 2011; Mallet 2007; Pollard et al. 2006).

473 Using RAD-sequencing data, the assignment of samples into species was concordant
474 with morphology (Fig. 1b,c and S4b,c) and we did not detect significant levels of
475 contemporary gene flow using population genetics-based approaches (Fig. 1d), despite
476 apparent opportunities for hybridization. Most of *Chiastocheta* occur in sympatry (Fig.
477 S1), they also have very similar biologies, reproducing and spending most of their time
478 on or inside flowers of *Trollius europaeus* (Pellmyr 1989; Suchan et al. 2015). Although a
479 temporal sequence in oviposition has been observed (Després & Jaeger 1999;

480 Johannesen & Loeschcke 1996; Pellmyr 1989), most species co-occur temporally.
481 Despite these ecological similarities and the relatively young age of the genus (most of
482 the clades emerging less than 1.6 Ma; Espindola et al. 2012), a lack of nuclear evidence
483 for hybridization indicates strong contemporary reproductive barriers among the
484 species.

485 5. Conclusions

486 This study demonstrates how a combination of RAD-seq and mtDNA data can provide
487 insights into phylogenies of genera that are poorly resolved using mitochondrial
488 markers alone and reveal complex picture of mitonuclear discordance. It also
489 underlines the limits of RAD-seq-based phylogenies in case of rapid radiations. Our
490 results show that a scenario of rapid radiation can affect many loci across the genome,
491 leading to discordant gene trees, even when using methods controlling for incomplete
492 lineage sorting. This may point to an inherent limitation of using molecular markers to
493 resolve rapid radiations, at least at some of the inter-specific relationships, and suggests
494 that this limitation is not necessarily due to technical issues (e.g. low number of shared
495 markers).

496 Adding to the body of examples of mito-nuclear discordance (reviewed in Toews &
497 Brelsford 2012), our study warns against relying solely on mitochondrial markers (e.g.,
498 COI barcoding; Herbert et al. 2003) for species delimitation, especially when they show
499 incongruence with classical taxonomy. In the case presented here, mitochondrial
500 markers suggested poly- or paraphyly for most species, and proposed the need to
501 review the taxonomy of the genus (Espíndola et al. 2012). When tackled from the
502 genomic point of view, the genetic support of species status for these seven entities was

503 confirmed. Finally, we provide an example of how ML phylogenies based on large
504 concatenated datasets can provide erroneously high bootstrap supports for incorrect or
505 uncertain topologies (Giarla & Esselstyn 2015; Kubatko & Degnan 2007).

506 Acknowledgments

507 The authors would like to thank Y. Triponez, N. Magrou, P. Lazarevic, D. Gyurova, R.
508 Lavigne, L. Juillerat, N. Villard, and R. Arnoux for their help during the fieldwork and V.
509 Michelsen for his great help with species determination. We also thank J. Ollerton and J.
510 Pannell for insightful discussions and comments on the manuscript. This work was
511 supported by the grant ‘Fonds des Donations’ of the University of Neuchâtel
512 (Switzerland) attributed to AE. TS acknowledges funding from the Rectors’ Conference
513 of the Swiss Universities (CRUS) through the “Scientific Exchange Program between
514 Switzerland and the new EU member states” (Sciex NMS grant no. 10.116) and from
515 Société Académique Vaudoise (Switzerland). This work was funded by the Swiss
516 National Science Foundation (grants 3100A0-116778, PZ00P3-126624,
517 PP00P3_144870 to N. Alvarez, and grant PP00P3_150654 to CD) and by a grant from
518 Switzerland through the Swiss Contribution to the enlarged European Union (Polish-
519 Swiss Research Program, project no. PSPB-161/2010).

520 References

- 521 Andrews KR, Good JM, Miller MR, Luikart G, Hohenlohe PA (2016) Harnessing the
522 power of RADseq for ecological and evolutionary genomics. *Nature Reviews*
523 *Genetics*, 17, 81-92.
- 524 Anisimova M, Gil M, Dufayard J-F, Dessimoz C, Gascuel O (2011) Survey of Branch
525 Support Methods Demonstrates Accuracy, Power, and Robustness of Fast
526 Likelihood-based Approximation Schemes. *Systematic Biology*, 60, 685–699.
- 527 Avise JC, Robinson TJ, Kubatko L (2008) Hemiplasy: a new term in the lexicon of
528 phylogenetics. *Systematic Biology*, 57(3), 503-507.
- 529 Baird NA, Etter PD, Atwood TS, Currey MC, Shiver AL, Lewis ZA, Selker EU, Cresko WA,
530 Johnson EA (2008) Rapid SNP discovery and genetic mapping using sequenced RAD
531 markers. *PLoS ONE*, 3, e3376.
- 532 Ballard JWO (2000) When one is not enough: introgression of mitochondrial DNA in
533 *Drosophila*. *Molecular Biology and Evolution*, 17, 1126-1130.
- 534 Ballard JWO, Melvin RG, Katewa SD, Maas K (2007) Mitochondrial DNA variation is
535 associated with measurable differences in life-history traits and mitochondrial
536 metabolism in *Drosophila simulans*. *Evolution*, 61, 1735-1747.
- 537 Ballard JWO, Pichaud N (2014) Mitochondrial DNA: more than an evolutionary
538 bystander. *Functional Ecology*, 28, 218-231.
- 539 Ballard JWO, Whitlock MC (2004) The incomplete natural history of mitochondria.
540 *Molecular Ecology*, 13, 729-744.

541 Birky CW (2001) The inheritance of genes in mitochondria and chloroplasts: laws,
542 mechanisms, and models. *Annual Review of Genetics*, 35, 125-48.

543 Boratyński Z, Melo-Ferreira J, Alves PC, Berto S, Koskela E, Pentikäinen OT, Mappes T
544 (2014) Molecular and ecological signs of mitochondrial adaptation: consequences
545 for introgression. *Heredity*, 113, 277-286.

546 Brelsford A, Milá B, Irwin DE (2011) Hybrid origin of Audubon's warbler. *Molecular*
547 *Ecology*, 20, 2380-2389.

548 Cariou M, Duret L, Charlat S (2013) Is RAD-seq suitable for phylogenetic inference? An
549 *in silico* assessment and optimization. *Ecology and Evolution*, 3, 846-852.

550 Chattopadhyay B, Garg KM, Ramakrishnan U (2014) Effect of diversity and missing data
551 on genetic assignment with RAD-Seq markers. *BMC research notes*, 7, 841.

552 Chifman J, Kubatko L (2014) Quartet inference from SNP data under the coalescent
553 model. *Bioinformatics*, 30:3317-3324.

554 Collin JE (1954) The genus *Chiastocheta* Pokorny (Diptera: Anthomyiidae). *Proceedings*
555 *of the Royal Entomological Society London (B)*, 23, 95-102.

556 Combosch DJ, Vollmer SV (2015) Trans-Pacific RAD-Seq population genomics confirms
557 introgressive hybridization in Eastern Pacific *Pocillopora* corals. *Molecular*
558 *Phylogenetics and Evolution*, 88, 154-162.

559 Cruaud A, Gautier M, Galan M, Foucaud J, Sauné L, Genson G, Rasplus JY (2014)
560 Empirical assessment of RAD sequencing for interspecific phylogeny. *Molecular*
561 *Biology and Evolution*, 31, 1272-1274.

562 DaCosta JM, Sorenson MD (2016) ddRAD-seq phylogenetics based on nucleotide, indel,
563 and presence–absence polymorphisms: Analyses of two avian genera with
564 contrasting histories. *Molecular Phylogenetics and Evolution*, 94, 122-135.

565 Davey JL, Blaxter MW (2010) RADSeq: Next-generation population genetics. *Briefings in*
566 *Functional Genomics*, 9, 416-423.

567 Davey JW, Hohenlohe PA, Etter PD, Boone JQ, Catchen JM, Blaxter ML (2011) Genome-
568 wide genetic marker discovery and genotyping using next-generation sequencing.
569 *Nature Reviews Genetics*, 12, 499-510.

570 DeFilippis VR, Moore WS (2000) Resolution of phylogenetic relationships among
571 recently evolved species as a function of amount of DNA sequence: An empirical
572 study based on woodpeckers (Aves: Picidae). *Molecular Phylogenetics and*
573 *Evolution*, 16, 143-160.

574 Degnan, J.H., Rosenberg, N.A., 2009. Gene tree discordance, phylogenetic inference and
575 the multispecies coalescent. *Trends in Ecology and Evolution* 24, 332–340.

576 Després L, Jaeger N (1999) Evolution of oviposition strategies and speciation in the
577 globeflower flies *Chiastocheta* spp. (Anthomyiidae). *Journal of Evolutionary Biology*,
578 12, 822-831.

579 Després L, Pettex E, Plaisance V, Pompanon F (2002) Speciation in the globeflower fly
580 *Chiastocheta* spp. (Diptera: Anthomyiidae) in relation to host plant species,
581 biogeography, and morphology. *Molecular Phylogenetics and Evolution*, 22, 258-268.

582 Dowling DK, Friberg U, Lindell J (2008) Evolutionary implications of non-neutral
583 mitochondrial genetic variation. *Trends in Ecology and Evolution*, 23, 546-554.

584 Earl DA, vonHoldt BM (2012) STRUCTURE HARVESTER: a website and program for
585 visualizing STRUCTURE output and implementing the Evanno method. *Conservation*
586 *Genetics Resources*, 4, 359-361.

587 Eaton DAR (2014) PyRAD: assembly of de novo RADseq loci for phylogenetic analyses.
588 *Bioinformatics*, 30, 1844-1849.

589 Eaton DAR, Ree RH (2013) Inferring phylogeny and introgression using genomic
590 RADseq data: An example from flowering plants (*Pedicularis*: Orobanchaceae).
591 *Systematic Biology*, 62, 689-706.

592 Eaton, D. A., Spriggs, E. L., Park, B., & Donoghue, M. J. (2016). Misconceptions on Missing
593 Data in RAD-seq Phylogenetics with a Deep-scale Example from Flowering Plants.
594 *Systematic Biology*, syw092.

595 Edgar RC (2004) MUSCLE: multiple sequence alignment with high accuracy and high
596 throughput. *Nucleic Acids Research* 32, 1792-1797.

597 Escudero M, Eaton DA, Hahn M, Hipp AL (2014) Genotyping-by-sequencing as a tool to
598 infer phylogeny and ancestral hybridization: A case study in *Carex* (Cyperaceae).
599 *Molecular Phylogenetics and Evolution*, 79, 359-367.

600 Espíndola A, Buerki S, Alvarez N (2012) Ecological and historical drivers of
601 diversification in the fly genus *Chiastocheta* Pokorny. *Molecular Phylogenetics and*
602 *Evolution*, 63, 466-474.

603 Evanno G, Regnaut S, Goudet J (2005) Detecting the number of clusters of individuals
604 using the software STRUCTURE: a simulation study. *Molecular Ecology*, 14, 2611-
605 2620.

606 Faircloth BC, Branstetter MG, White ND, Brady SG (2014) Target enrichment of
607 ultraconserved elements from arthropods provides a genomic perspective on
608 relationships among Hymenoptera. *Molecular Ecology Resources*, 15, 489-501

609 Funk DJ, Omland KE (2003) Species-level paraphyly and polyphyly: frequency, causes,
610 and consequences, with insights from animal mitochondrial DNA. *Annual Review of*
611 *Ecology, Evolution and Systematics*, 34, 397-423.

612 Gatesy, J, Springer MS (2013) Concatenation versus coalescence versus
613 “concatalescence”. *Proceedings of the National Academy of Sciences*, 110, E1179-
614 E1179.

615 Gautier M, Gharbi K, Cezard T, Foucaud J, Kerdelhué C, Pudlo P, Cornuet J-M, Estoup A
616 (2013) The effect of RAD allele dropout on the estimation of genetic variation
617 within and between populations. *Molecular Ecology*, 22, 3165-3178.

618 Giarla TC, Esselstyn JA (2015) The challenges of resolving a rapid, recent radiation:
619 Empirical and simulated phylogenomics of philippine shrews. *Systematic Biology*,
620 64, 727-740.

621 Gori K, Suchan T, Alvarez N, Goldman N, Dessimoz C (2016) Clustering genes of common
622 evolutionary history. *Molecular Biology and Evolution*, 33,1590–1605

623 Govindarajulu R, Parks M, Tennessen JA, Liston A, Ashman TL (2015) Comparison of
624 nuclear, plastid, and mitochondrial phylogenies and the origin of wild octoploid
625 strawberry species. *American Journal of Botany*, 102, 544-554.

- 626 Harvey MG, Judy CD, Seeholzer GF, Maley JM, Graves GR, Brumfield RT (2015) Similarity
627 thresholds used in DNA sequence assembly from short reads can reduce the
628 comparability of population histories across species. *PeerJ*, 3, e895.
- 629 Harvey MG, Smith BT, Glenn TC, Faircloth BC, Brumfield RT (2016) Sequence capture
630 versus restriction site associated DNA sequencing for shallow systematics.
631 *Systematic Biology*, 65, 910-924.
- 632 Hebert PDN, Cywinska A, Ball SL, deWaard JR (2003) Biological identifications through
633 DNA barcodes. *Proceedings of the Royal Society B: Biological Sciences*, 270, 313-322.
- 634 Hennig W (Ed.) (1976) Anthomyiidae. Die Fliegen der Palaearktischen Region. Stuttgart,
635 E. Schweizerbart.
- 636 Herrera S, Shank TM (2016) RAD sequencing enables unprecedented phylogenetic
637 resolution and objective species delimitation in recalcitrant divergent taxa.
638 *Molecular Phylogenetics and Evolution*, 100, 70-79.
- 639 Hipp AL, Eaton DAR, Cavender-Bares J, Fitzek E, Nipper R, Manos PS (2014) A
640 framework phylogeny of the american oak clade based on sequenced RAD data.
641 *PLoS ONE*, 9, e93975.
- 642 Hovmöller R, Knowles LL, Kubatko LS (2013) Effects of missing data on species tree
643 estimation under the coalescent. *Molecular Phylogenetics and Evolution*, 69, 1057-
644 1062.
- 645 Huang H, Knowles LL (2014) Unforeseen consequences of excluding missing data from
646 next-generation sequences: simulation study of RAD sequences. *Systematic Biology*,
647 doi:10.1093/sysbio/syu046.

648 Ilut DC, Nydam ML, Hare MP (2014) Defining loci in restriction-based reduced
649 representation genomic data from nonmodel species: Sources of bias and
650 diagnostics for optimal clustering. *BioMed Research International*, 2014, 675158.

651 Johannesen J, Loeschcke V (1996) Distribution, abundance and oviposition patterns of
652 four coexisting *Chiastocheta* species (Diptera: Anthomyiidae). *Journal of Animal*
653 *Ecology*, 65, 567-576.

654 Jones JC, Fan S, Franchini P, Schartl M, Meyer A (2013) The evolutionary history of
655 *Xiphophorus* fish and their sexually selected sword: a genome-wide approach using
656 restriction site-associated DNA sequencing. *Molecular Ecology*, 22, 2986-3001.

657 Kubatko LS, Degnan JH (2007) Inconsistency of phylogenetic estimates from
658 concatenated data under coalescence. *Systematic Biology*, 56, 17-24.

659 Lanfear R, Frandsen PB, Wright AM, Senfeld T, Calcott B (2017) PartitionFinder 2: new
660 methods for selecting partitioned models of evolution for molecular and
661 morphological phylogenetic analyses. *Molecular Biology and Evolution*. 34, 772-773.

662 Leaché AD, Chavez AS, Jones LN, Grummer JA, Gottscho AD, Linkem CW (2015)
663 Phylogenomics of phrynosomatid lizards: conflicting signals from sequence capture
664 versus restriction site associated DNA sequencing. *Genome Biology and Evolution*, 7,
665 706-719.

666 Leaché AD, Harris RB, Rannala B, Yang Z (2013) The influence of gene flow on species
667 tree estimation: a simulation study. *Systematic Biology*, 63, 17-30.

668 Lowry DB, Hoban S, Kelley JL, Lotterhos KE, Reed LK, Antolin MF, Storfer A (2017)
669 Breaking RAD: an evaluation of the utility of restriction site-associated DNA

670 sequencing for genome scans of adaptation. *Molecular Ecology Resources*, 17, 142–
671 152.

672 Maddison WP (1997) Gene trees in species trees. *Systematic Biology*, 46, 523-536.

673 Maddison WP, Knowles LL (2006) Inferring phylogeny despite incomplete lineage
674 sorting. *Systematic Biology*, 55, 21-30.

675 Mallet J (2007) Hybrid speciation. *Nature*, 446, 279-283.

676 Manthey JD, Campillo LC, Burns KJ, Moyle RG (2016) Comparison of target-capture and
677 restriction-site associated DNA sequencing for phylogenomics: a test in cardinalid
678 tanagers (Aves, Genus: *Piranga*). *Systematic biology*, syw005.

679 Mastretta-Yanes A, Zamudio S, Jorgensen TH, Arrigo N, Alvarez N, Piñero D, Emerson BC
680 (2014) Gene duplication, population genomics, and species-level differentiation
681 within a tropical mountain shrub. *Genome biology and evolution*, 6, 2611-2624.

682 Mastretta-Yanes A, Arrigo N, Alvarez N, Jorgensen TH, Piñero D, Emerson BC (2015)
683 Restriction site-associated DNA sequencing, genotyping error estimation and de
684 novo assembly optimization for population genetic inference. *Molecular Ecology*
685 *Resources*, 15, 28-41.

686 McCormack JE, Faircloth BC, Crawford NG, Gowaty PA, Brumfield RT, Glenn TC (2012)
687 Ultraconserved elements are novel phylogenomic markers that resolve placental
688 mammal phylogeny when combined with species tree analysis. *Genome Research*,
689 22, 746-754.

690 McKinney GJ, Larson WA, Seeb LW, Seeb JE (2017) RADseq provides unprecedented
691 insights into molecular ecology and evolutionary genetics: comment on Breaking
692 RAD by Lowry *et al.* (2016). *Molecular Ecology Resources*, doi:10.1111/1755-
693 0998.12649.

694 Michelsen V (1985) A revision of the Anthomyiidae (Diptera) described by J.W.
695 Zetterstedt. *Steenstrupia*, 11, 37-65

696 Miller MA, Pfeiffer W, Schwartz T (2010) Creating the CIPRES Science Gateway for
697 inference of large phylogenetic trees. In: Proceedings of the Gateway Computing
698 Environments Workshop (GCE), 14 Nov. 2010, New Orleans, LA pp. 1-8.

699 Nadeau NJ, Martin SH, Kozak KM, Salazar C, Dasmahapatra K, Davey JW, Baxter SW,
700 Blaxter ML, Mallet J, Jiggins CD (2013) Genome-wide patterns of divergence and
701 gene flow across a butterfly radiation. *Molecular Ecology*, 22, 814–826.

702 Pante E, Abdelkrim J, Viricel A, Gey D, France SC, Boisselier MC, Samadi S (2015) Use of
703 RAD sequencing for delimiting species. *Heredity*, 114, 450-459.

704 Paradis E, Claude J, Strimmer K (2004) APE: analyses of phylogenetics and evolution in
705 R language. *Bioinformatics*, 20, 289-290.

706 Pellmyr O (1989) The cost of mutualism – interactions between *Trollius europaeus* and
707 its pollinating parasites. *Oecologia*, 78, 53-59.

708 Pellmyr O (1992) The phylogeny of a mutualism: evolution and coadaptation between
709 *Trollius* and its seed-parasitic pollinators. *Biological Journal of the Linnean Society*,
710 47, 337-365.

711 Peterson BK, Weber JN, Kay EH, Fisher HS, Hoekstra HE (2012) Double digest RADseq:
712 An inexpensive method for de novo SNP discovery and genotyping in model and
713 non-model species. *PLoS ONE*, 7, e37135.

714 Phillips MJ, Haouchar D, Pratt RC, Gibb GC, Bunce M (2013) Inferring Kangaroo
715 Phylogeny from Incongruent Nuclear and Mitochondrial Genes. *PLoS ONE*, 8,
716 e57745.

717 Pollard DA, Iyer VN, Moses AM, Eisen MB (2006) Widespread discordance of gene trees
718 with species tree in *Drosophila*: Evidence for incomplete lineage sorting. *PLoS*
719 *Genetics*, 2, e173.

720 Pritchard JK, Stephens M, Donnelly P (2000) Inference of population structure using
721 multilocus genotype data. *Genetics*, 155, 945-959.

722 Reaz R, Bayzid MS, Rahman MS (2014) Accurate phylogenetic tree reconstruction from
723 quartets: A heuristic approach. *PloS One*, 9:e104008.

724 Roch S, Warnow T (2015) On the robustness to gene tree estimation error (or lack
725 thereof) of coalescent-based species tree methods. *Systematic Biology*, syv016.

726 Rokas A, Carroll SB (2005) More genes or more taxa? The relative contribution of gene
727 number and taxon number to phylogenetic accuracy. *Molecular Biology and*
728 *Evolution*, 22, 1337-1344.

729 Rubin BER, Ree RH, Moreau CS (2012) Inferring phylogenies from RAD sequence data.
730 *PLoS ONE*, 7, e33394.

731 Rubinoff D, Holland BS (2005) Between two extremes: mitochondrial DNA is neither the
732 panacea nor the nemesis of phylogenetic and taxonomic inference. *Systematic*
733 *Biology*, 54, 952-961.

734 Schmid S, Genevest R, Gobet E, Suchan T, Sperisen C, Tinner W, Alvarez N (2017)
735 HyRAD-X, a versatile method combining exome capture and RAD sequencing to
736 extract genomic information from ancient DNA. *Methods in Ecology and Evolution*,
737 doi:10.1111/2041-210X.12785

738 Seehausen O, Koetsier E, Schneider MV, Chapman LJ, Chapman CA, Knight ME, Turner
739 GF, van Alphen JJM, Bills R (2003) Nuclear markers reveal unexpected genetic
740 variation and a Congolese-Nilotic origin of the Lake Victoria cichlid species flock.
741 *Proceedings of the Royal Society of London Series B*, 270, 129-137.

742 Springer MS, Gatesy J (2016) The gene tree delusion. *Molecular Phylogenetics and*
743 *Evolution*, 94, 1-33.

744 Stamatakis A (2014) RAxML Version 8: A tool for phylogenetic analysis and post-
745 analysis of large phylogenies. *Bioinformatics*, 30, 1312-1313.

746 Suchan T, Beauverd M, Trim N, Alvarez N (2015) Asymmetrical nature of the *Trollius-*
747 *Chiastocheta* interaction: insights into the evolution of nursery pollination systems.
748 *Ecology and Evolution*, 5, 4766-4777.

749 Suchan T, Pitteloud C, Gerasimova NS, Kostikova A, Schmid S, Arrigo N, Pajkovic M,
750 Ronikier M, Alvarez N (2016) Hybridization Capture Using RAD Probes (hyRAD), a
751 New Tool for Performing Genomic Analyses on Collection Specimens. *PLoS ONE*, 11,
752 e0151651.

753 Suchan T, Espíndola A, Rutschmann S, Emerson BC, Gori K, Dessimoz C, Arrigo N, Ronikier
754 M, Alvarez N (2017) Data from: Assessing the potential of RAD-sequencing to resolve phy-
755 logenetic relationships within species radiations: the fly genus *Chiastocheta* (Diptera: An-
756 thomyiidae) as a case study. *Mendeley Data*, <https://doi.org/XXX>

757 Swofford DL (2002) PAUP*: Phylogenetic analysis using parsimony (*and other
758 methods). Version 4. Sinauer, Sunderland, Massachusetts, USA.

759 Toews DP, Brelsford A (2012) The biogeography of mitochondrial and nuclear
760 discordance in animals. *Molecular Ecology*, 21, 3907-3930.

761 Townsend TM, Mulcahy DG, Noonan BP, Sites JW, Kuczynski CA, Wiens JJ, Reeder TW
762 (2011) Phylogeny of iguanian lizards inferred from 29 nuclear loci, and a
763 comparison of concatenated and species-tree approaches for an ancient, rapid
764 radiation. *Molecular Phylogenetics and Evolution*, 61, 363-380.

765 Wagner CE, Keller I, Wittwer S, Selz OM, Mwaiko S, Greuter L, Sivasundar A, Seehausen
766 O (2013) Genome-wide RAD sequence data provide unprecedented resolution of
767 species boundaries and relationships in the Lake Victoria cichlid adaptive radiation.
768 *Molecular Ecology*, 22, 787-798.

769 Walsh HE, Kidd MG, Moum T, Friesen VL (1999) Polytomies and the power of
770 phylogenetic inference. *Evolution*, 53, 932-937.

771 Whitfield JB, Kjer KM (2008) Ancient rapid radiations of insects: challenges for
772 phylogenetic analysis. *Annual Review of Entomology*, 53, 449-472.

773 Whitfield JB, Lockhart PJ (2007) Deciphering ancient rapid radiations. *Trends in*
774 *Ecology and Evolution*, 22, 258-265.

- 775 Wielstra B, Arntzen JW, van der Gaag KJ, Pabijan M, Babik W (2014) Data Concatenation,
776 Bayesian Concordance and Coalescent-Based Analyses of the Species Tree for the
777 Rapid Radiation of *Triturus* Newts. *PLoS ONE*, 9, e111011.
- 778 Williams JS, Niedzwiecki JH, Weisrock DW (2013) Species tree reconstruction of a
779 poorly resolved clade of salamanders (Ambystomatidae) using multiple nuclear
780 loci. *Molecular Phylogenetics and Evolution*, 68, 671-682.
- 781 Zetterstedt JW (1845) *Diptera scandinaviae disposita et descripta*. IV, 1281-1738. Lund,
782 Sweden.
- 783 Zink RM, Barrowclough GF (2008) Mitochondrial DNA under siege in avian
784 phylogeography. *Molecular Ecology*, 17, 2107-2121.

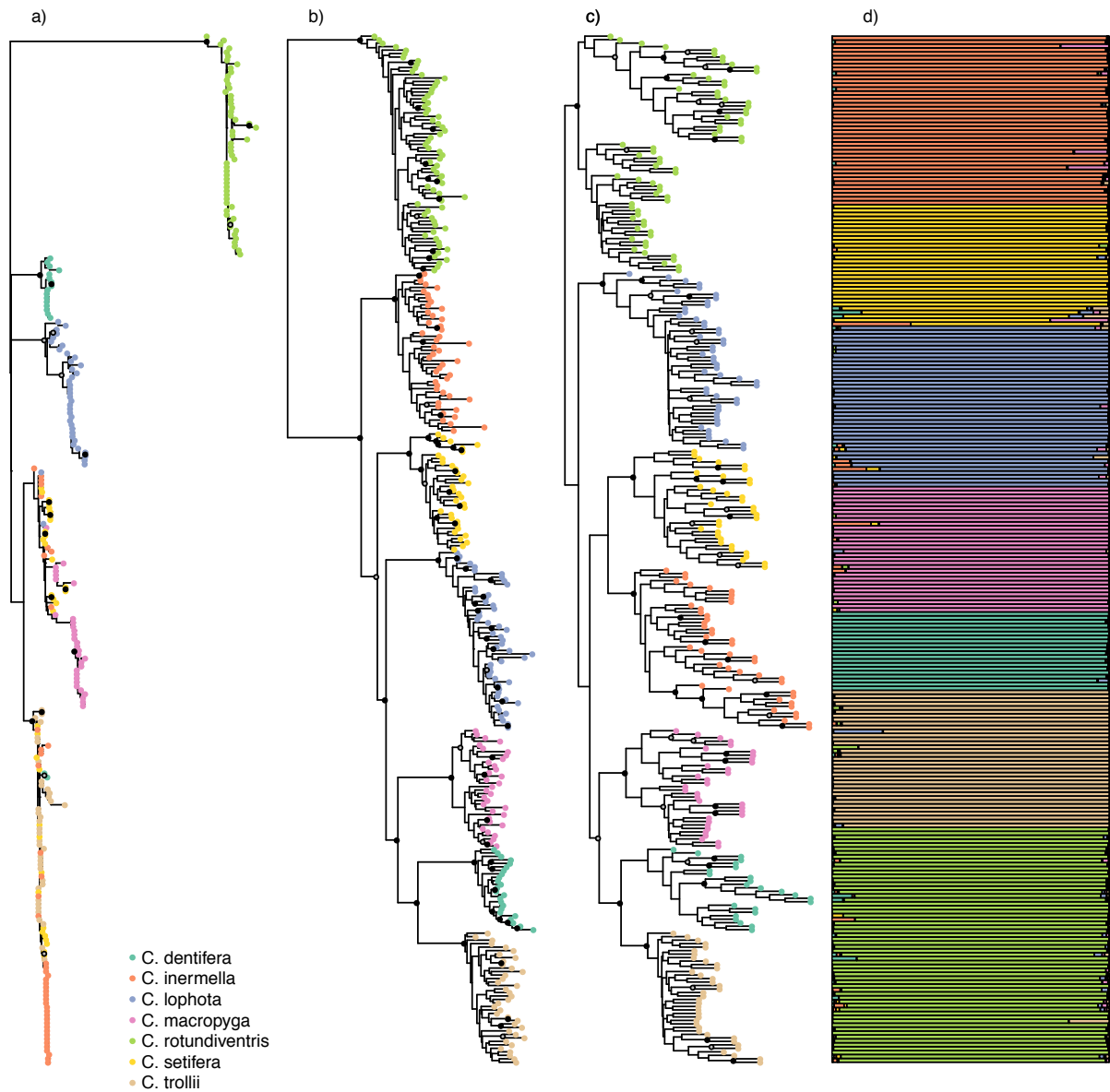
785 Data Accessibility

786 DNA sequences are available on Genbank under accessions no XXX-XXX. Nexus and
787 STRUCTURE datasets used for the analyses, ML phylogeny inferred for the main RAD
788 dataset, SVDquartet analyses, and ML phylogeny inferred for the mtDNA dataset are
789 available on Mendeley Data <https://doi.org/XXX> (Suchan et al. 2017).

790 Author Contributions

791 TS, NA, AE, KG and CD designed research, TS, AE, KG, and SR performed research and
792 analyzed data. All authors wrote the paper.

793 Figures



794

795

796

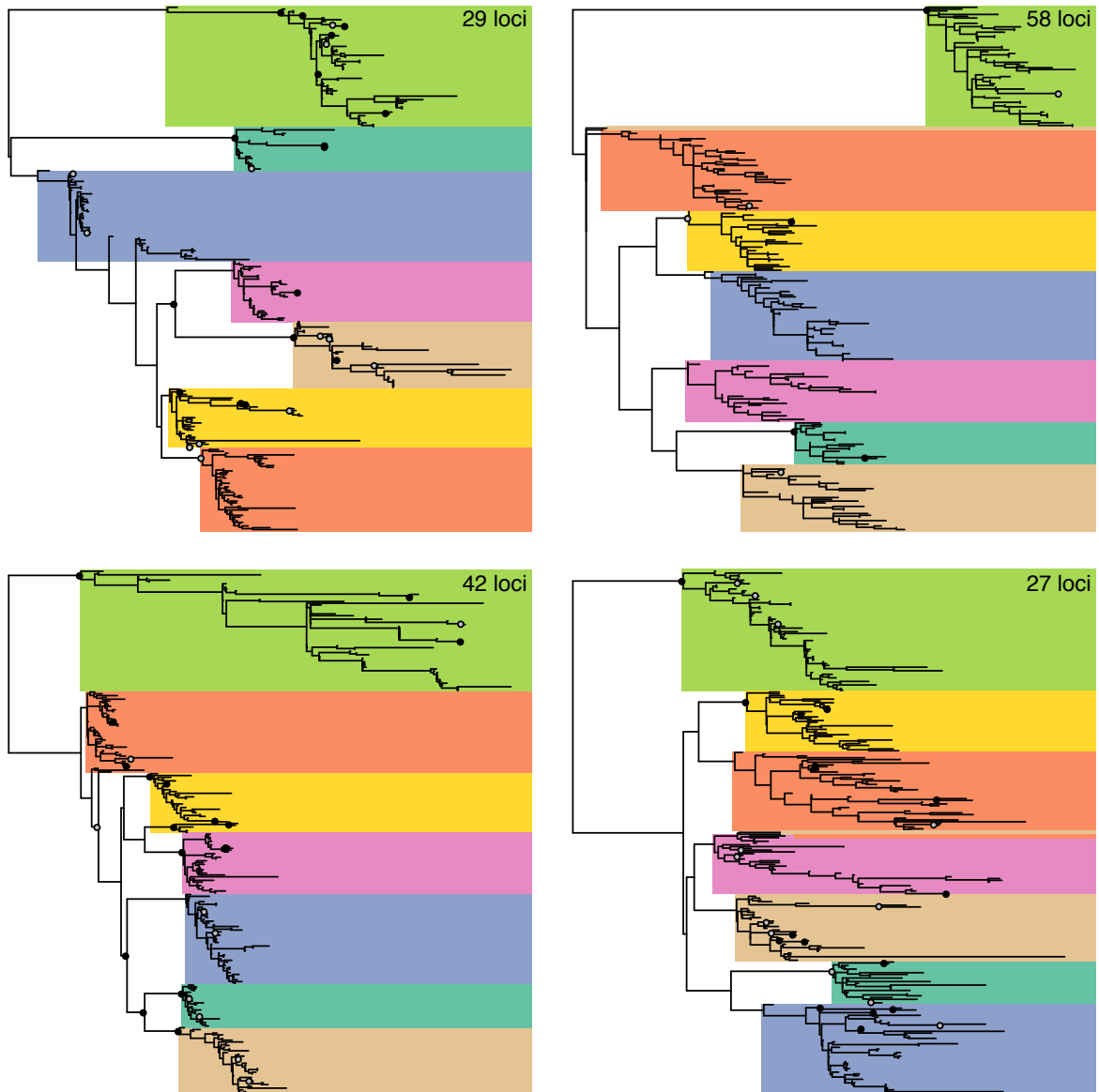
797

798

799

800

Figure 1. Phylogenies obtained for a) ML analysis of the mtDNA dataset; b) ML analysis of the RAD dataset; c) SVDquartets analysis of RAD dataset; bootstrap node supports > 80 are shown denoted by gray points, bootstrap node supports > 90 are shown denoted by black points. d) Population clustering of the sampled *Chiastocheta* specimens, estimated with STRUCTURE using $K = 7$ value.



801

802

803 Figure 2. Phylogenetic trees on the four bins, as identified by the treeCl analysis,

804 considering only the loci present in at least 100 specimens. Bootstrap node supports >

805 80 are shown denoted by gray points, bootstrap node supports > 90 are shown denoted

806 by black points.

807 Tables

808 Table 1. Populations included in the study, with geographical coordinates and the
809 number of specimens used in the final analyses. Letter codes denote *Chiastocheta*
810 species: *C. dentifera* (D), *C. inermella* (I), *C. lophota* (L), *C. macropyga* (M), *C.*
811 *rotundiventris* (R), *C. setifera* (S), and *C. trollii* (T).

code	site	latitude	longitude	year	D	I	L	M	R	S	T	sum
AMB	Ambri	46.50680	8.70292	2008			2	4	2		1	9
AMO	Amot	59.62199	8.42346	2007		4						4
BAY	Bayasse	44.30814	6.74067	2007		1	2	2	2		3	10
BEI	Beistohlen	61.20761	8.95473	2007		5						5
BID	Bidjovagge	69.29778	22.47808	2008		1			1			2
BON	Col de Bonnecombe	44.57557	3.11410	2007				3	1	1	2	7
BRA	Braas	57.09309	15.06817	2007		1						1
CCO	Col de la Co- lombière	45.98722	6.46972	2006			2	1	2		1	6
CDV	Creux du Van	46.93526	6.74119	2006		1	2		2	2		7
CHA	Chasseral	47.12569	7.02130	2006			5		3		1	9
CHE	Chemin	46.08993	7.08978	2006	3	1		3	2	1	2	12
CRA	Crans-Montana	46.34650	7.53890	2006		1	1		3	1	1	7
CRE	Cressbrook Dale	53.26724	-1.74041	2008						2		2
CTP	Colt Park	54.19365	-2.35247	2008		4			1		1	6
DON	Donovaly	48.88922	19.23068	2008			3	1	2			6
EID	Eidda Pastures	53.03720	-3.74190	2008						2		2
ELL	Ellingsrudelva	59.91771	10.91844	2007		1						1
EPO	Esposouille	42.62341	2.09450	2008	1		1		2	2	3	9
FRO	Froson	63.18205	14.60268	2007		2						2

GAL	Col du Galibier	45.08528	6.43861	2006		2	2		3		3	10
GLE	Glen Fender	56.78138	-3.79485	2008					2	2		4
HT1	Haute Tinee 1	44.29617	6.81871	2007			3					3
HT2	Haute Tinee 2	44.28426	6.85581	2007				3			1	4
KRA	Krasno Polje	44.80869	14.97271	2008						1		1
LAK	Laktatjakka	68.42931	18.40674	2007		1		4	2			7
LFE	Lough Fern	55.06569	-7.71130	2008						1		1
LOS	Loser	47.66052	13.78485	2007			4		3	1		8
MOE	Moerlimatt	47.90597	8.07760	2007			1		1	1	1	4
MTP	Monte Pizi	41.91524	14.16714	2008						2		2
NAV	Naverdal	62.70417	10.13002	2007		3					1	4
PAJ	Pajino Preslo	43.27799	20.81970	2008						2		2
PAN	Puerto de Panderrueda	43.12743	-4.97223	2008			1	1	3	2	1	8
PIL	Pila	48.90017	20.29449	2008	3		2	1				6
POD	Podlesok	48.94962	20.35190	2008				1			1	2
PPN	Petit Papa Noel	66.51647	25.79386	2007	1	3			2		3	9
PYD	Puy de Dome	45.77222	2.96333	2006			2	2	2			6
PYM	Puy Mary	45.11139	2.68083	2006			1					1
PYS	Puy de Sancy	45.53500	2.80972	2006			3	2	1			6
RAD	Radkow	50.46866	16.35321	2008	2	4			2			8
RIS	Risnjak - Snjeznik	45.43871	14.58494	2008					1	2		3
SAL	Salla	66.83020	28.65427	2007	1				2	1	4	8
SED	Sede de Pan	43.03949	-0.48651	2008			2					2
SET	Seterasen	65.53432	13.67744	2007	1	4		1	1		1	8
SOL	Solberga	57.95194	13.56116	2007	4	2			2		1	9
STE	Steingaden	47.59529	11.01296	2007				1	1	31		5

STR	Straumen	67.38440	15.64921	2007					2			2
SUS	Susch	46.74728	10.07473	2006	2		2		2	1	3	10
SVA	Svartla	65.99583	21.22062	2007	3	3						6
TAR	Tarasp	46.77730	10.25056	2006			1		2	1	3	7
VIT	Vitosha	42.59032	23.29342	2008						2		2
ZAL	Zali Log	46.20342	14.11080	2008				3	2	1		6
				total:	21	44	42	33	59	34	38	271

812

813 Appendix A. Supplementary material

814 Table S1. Summary statistics for the RAD-sequenced samples: number of RAD
815 fragments clusters and mean coverage after retaining clusters with a coverage >5,
816 estimated heterozygosities, number of consensus loci after paralog filtering, and the
817 numbers of loci retained for each dataset after filtering for coverage among the samples.

818

819 Fig. S1. Map of the sampled *Chiastocheta* specimens used in the study.

820

821 Fig. S2. The effect of different clustering thresholds (*X*-axis) and minimum loci
822 coverages (indicated by colors: red – 10, blue – 20, green – 100 individuals) on the total
823 number of assembled loci, proportion of missing data, loci overlap among the technical
824 replicates, and mean number of individuals per locus.

825

826 Fig. S3. Pattern of RAD-seq loci sharing among the sequenced individuals for datasets:
827 a) the main dataset using clustering similarity of 75% and minimum loci coverage
828 among individuals of 20; b) using clustering similarity of 75% and minimum loci
829 coverage among individuals of 100.

830

831 Fig. S4. a) ML phylogeny inferred for the mtDNA dataset; b) ML phylogeny inferred for
832 the RAD-seq dataset; c) SVDquartets phylogeny inferred for the RAD-seq dataset;
833 bootstrap node supports > 80 are shown denoted by gray points, bootstrap node
834 supports > 90 are shown denoted by black points.

835

836 Fig. S5. STRUCTURE runs for $K=2$ to 7, plotted against the RAD-seq based phylogeny.

837 Fig. S6. Phylogenetic trees on the loci partitioned into the sets of 2 to 6 clusters,
838 considering only the loci present in at least 100 specimens. Bootstrap node supports >
839 80 are shown denoted by gray points, bootstrap node supports > 90 are shown denoted
840 by black points. Numbers below the trees denote the number of clusters into which the
841 dataset was divided. Plot of log-likelihood improvement versus the number of clusters
842 is presented in the first box.

843

844 Appendix S1. RAD-sequencing protocol.